Scaling Laws for Hall Thruster Performance

A. Fruchtman

Center for Technological Education Holon
52 Golomb St., P.O. Box 305
Holon 58102, Israel

N. J. Fisch

Princeton Plasma Physics Laboratory
Princeton University, P.O. Box 451
Princeton, NJ 08543, USA

J. Ashkenazy and Y. Raitses

Propulsion Physics Laboratory
Soreq NRC
Yavne 81800, Israel

Abstract

A simple theoretical model of the Hall thruster is presented. Dimensionless parameters that determine the thruster performance are identified. The simplicity of the model enables us to explore easily parametric dependencies of the discharge features and the thruster performance. A good agreement is found between the predictions of the model and the experimental measurements.

I. Introduction

Since the introduction of the Hall thruster concept,[1,2] there has been a continuous effort to explore the dependence of the thrust, the specific impulse, and the efficiency on various parameters, such as thruster dimensions, magnetic field, applied voltage, ion mass, electron conductivity, and gas mass flow rate.[3–17] It would be useful, however, to have a simple theoretical model, identifying dimensionless parameters that govern the thruster performance. A fast parametric study could then be easily performed.

We begin by employing a one-dimensional steady-state model, including a cold-fluid description of the ions with an effective drag term due to ion production. The same model was explored numerically by Manzella.[11] We note a singularity in the equations due to the presence of the sonic transition. The electron dynamics, described by Ohm's law, is governed by the magnetic field, the electron pressure, and collisions across the magnetic field. For simplicity, we assume here that the electron temperature is uniform along the thruster, and we neglect wall losses. We look for steady state solutions where the axial dependence of the radial magnetic field, the thruster dimensions, the applied voltage, the mass flow rate, the neutral axial velocity, and the electron temperature are specified. We also assume that the ion current at the anode is zero, corresponding to a monotonically decreasing potential from the anode to the cathode. We then solve for the axial dependence of the electric potential, the plasma and the neutral densities, the electron and the ion currents. The discharge current is determined by the requirement of regularity and smoothness of the solutions through the sonic transition plane.

In Sec. II we present the governing equations.

In Sec. III we discuss the meaning of the governing dimensionless parameters. Solutions of the equations are presented in Sec. IV for various values of the dimensionless parameters. The calculations are compared with experimental results in Sec. V.

II. The governing equations

Let us first present the governing equations. For the dimensionless ion (and electron) density $N = n_e v_0 MA/\dot{m}$, ion current $J \equiv j_i MA/e\dot{m}$, and electric potential $\psi \equiv \phi/\phi_A$ (ϕ_A is the applied voltage) as a function of the normalized coordinate $\xi \equiv x/L$. The ion dynamics is governed by the ion momentum equation

$$N\frac{d\psi}{d\xi} + 2J\frac{d(J/N)}{d\xi} = -2pJ(1-J) , \qquad (1)$$

while the electron dynamics is governed by Ohm's law

$$\frac{(J_T - J)}{\mu} = -N\frac{d\psi}{d\xi} + t\frac{dN}{d\xi} . \qquad (2)$$

The ion continuity equation is

$$\frac{dJ}{d\xi} = pN(1-J) , \qquad (3)$$

where $pN(1-J)$ is the ionization rate. Quasi-neutrality is assumed. The ion velocity is expressed as J/N. The three parameters in the equations are

$$p \equiv \frac{L\beta\dot{m}}{v_a v_0 MA} , \qquad (4)$$

the dimensionless electron temperature

$$t \equiv T_e/e\phi_A , \qquad (5)$$

and the dimensionless electron mobility

$$\mu \equiv \frac{\nu_c}{m\omega_c^2 L}\left(\frac{eM\phi_A}{2}\right)^{1/2} . \qquad (6)$$

There is a fourth parameter, the dimensionless total current J_T. However, as we explain later, this parameter is not specified, but is rather determined by the solution.

In the above definitions, n_e is the electron (and ion) density, e is the elementary charge, L and A are the length and cross section of the thruster, $\dot{m}$ is the mass flow rate, v_a is the (assumed constant) neutral flow velocity, $v_0 \equiv (2e\phi_A/M)^{1/2}$, M and m are the ion and electron masses, T_e is the electron temperature, and x is the coordinate in the direction from the anode to the cathode. Also, ω_c is the electron cyclotron frequency, ν_c is the electron collision frequency. In the expression for p the parameter β is the average of σv, where σ is the ionization cross section. The electron mobility is the mobility across the magnetic field.

In writing the equations, we used current conservation, so the normalized electron current J_e can be written as $J_e = J_T - J$, where J_T is the total current. Also, the sum of the ion flux and the neutral flux J_n is constant along the thruster, i.e., $J + J_n = 1$. In our dimensionless units the propellant utilization is

$$\eta_m = J , \qquad (7a)$$

the current utilization is

$$\eta_C = \frac{J}{J_T} , \qquad (7b)$$

the energy utilization is

$$\eta_E = \frac{J^2}{N^2} , \qquad (7c)$$

and the total efficiency, therefore, is

$$\eta_T = \frac{J^4}{N^2 J_T} . \qquad (7d)$$

The normalized specific impulse is

$$I_{sp,N} \equiv \frac{J^2}{N} . \qquad (7e)$$

In the definitions (7a-7e), J and N are calculated at $\xi = 1$. Using Eq. (7e) we write the specific impulse as

$$I_{sp} = I_{sp,N}\frac{v_0}{g} . \qquad (7f)$$

and the thrust as

$$T = I_{sp,N}\dot{m}v_0 \ . \qquad (7g)$$

To Equations (1)–(3) for J, N and ψ, we add the boundary conditions: $\psi(0) = 1$, $\psi(1) = 0$ and $J(0) = 0$. The last boundary condition means that a monotonically decreasing potential from the anode towards the cathode is assumed and the possibility of a backwards ion flow towards the anode is excluded.

III. The dimensionless parameters

The behavior described in Eqs. (1)–(3) is governed by three dimensionless parameters: p, t, and μ. The electron temperature distribution is usually found by solving an appropriate energy equation. A major simplification is made here by assuming that the electron temperature is constant along the thruster. The temperature T_e affects not only the parameter t in the equations. More importantly, the ionization strongly depends on the temperature through the dependence of β. Also, the electron mobility depends on the electron temperature through the dependence of ν_c, arising from electron-atom, electron-wall,[10] electron-ion, and other collisions.

We also assume here that p is constant. The profile of the magnetic field is included by allowing μ to vary along the thruster axis. In the present work we assume that the dimensionless electron mobility is of the form

$$\mu = \mu_0 \exp\left[(L/d)^2(\xi - \xi_0)^2\right] \ . \qquad (8)$$

Another simplifying approximation is the neglect of the ion pressure in the momentum equation for the ions. Since ions are born through ionization along the thruster the ion pressure is not negligible. Ions are almost collisionless and there is no simple equation of state that relates their pressure to the lower moments. However, the theory can be generalized to describe the ions kinetically. In the present work, we do retain the ion production term through ionization, which appears as an effective drag term. The neglect of loss terms at the walls also simplifies, for the present, our analysis.

IV. Solution of the equations

Equations (1)–(3) are singular at the sonic transition point where the ion velocity equals the ion acoustic velocity. This is easily seen if Eqs. (1), (2) and (3) are combined to give

$$\left(2\frac{J^2}{N^2} - t\right)\frac{dN}{d\xi} = 4pJ(1-J) - \frac{(J_T - J)}{\mu} \ . \qquad (9)$$

In solving Eqs. (1)–(3), we choose to look for solutions that are regular at the sonic transition point. The requirement of regularity and the boundary conditions determine the value of the discharge current, J_T. While there are no firm theorems for either the uniqueness or existence of solutions, we do succeed, in practice, in finding regular solutions to Eqs. (1)–(3) with the specified boundary conditions.

The procedure of solution is the following: The equations are expanded analytically in the neighborhood of the assumed sonic transition point, and then integrated outward in both directions. The right-hand side (RHS) of Eq. (9) should be zero at the sonic transition point following the requirement of regularity at this point. The vanishing of the RHS determines the value of J_T. The location of the transition point is found by a shooting method, which assures also that the boundary conditions are satisfied.

The equations have been solved for fixed t and various values of p. For each value of p, the maximum efficiency is found by choosing the mobility μ_0 as small as possible, as long as solutions for the equations exist. This procedure roughly follows the experimental procedure of varying the mass flow rate (through variation of p) and then optimizing the efficiency by increasing the intensity of the magnetic field.

In the calculations presented here, $\xi_0 = 0.9$ and $(L/d)^2 = 5$, while the amplitude μ_0 is varied. A subsequent study will explore the influence of the mobility profile on the thruster performance. Figure 1 shows the spatial distribution of $\mu^{-1/2}$ for those values of ξ_0 and L/d. In the figure, $\mu_0 = 1$, but the profile simply scales up or down for other values of μ_0. This spatial profile is roughly the spatial profile of the magnetic field, which is precise if the collision frequency is uniform.

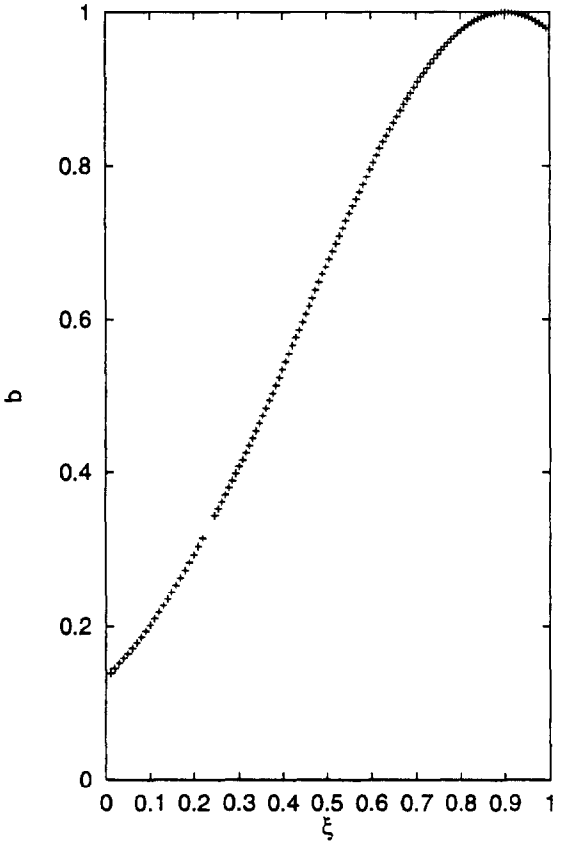

Fig. 1 The assumed magnetic field profile

Figures 2–7 show the features of the Hall thruster for two values of p and correspondingly two values of μ_0. Figure 2 shows the distribution of the electric potential. Figures 3 and 4 show the plasma density N and the ion current J for the two cases. Note that both the plasma density and the ion current are larger in the case that p is larger.

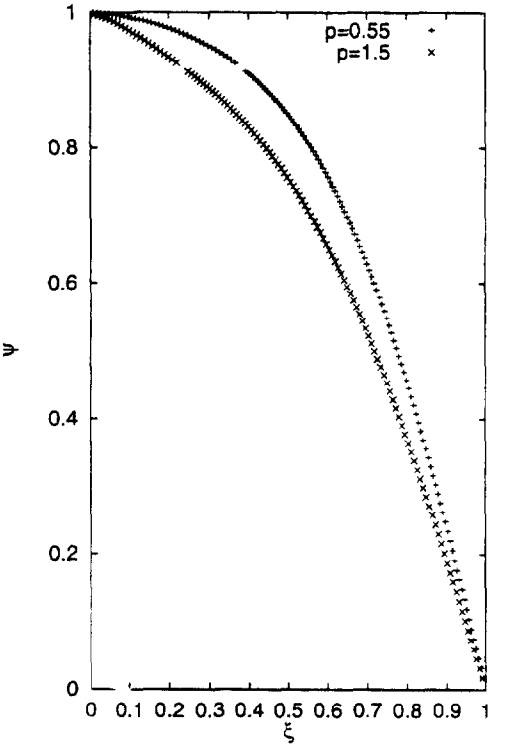

Fig. 2 The potential distribution

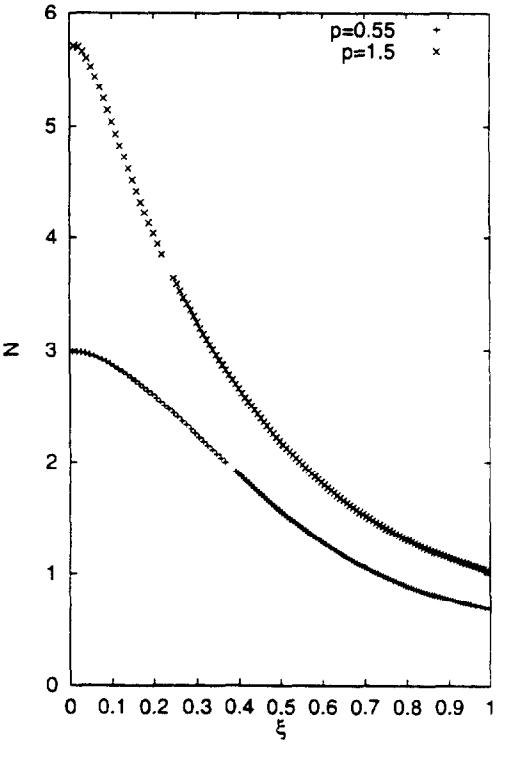

Fig. 3 The plasma density

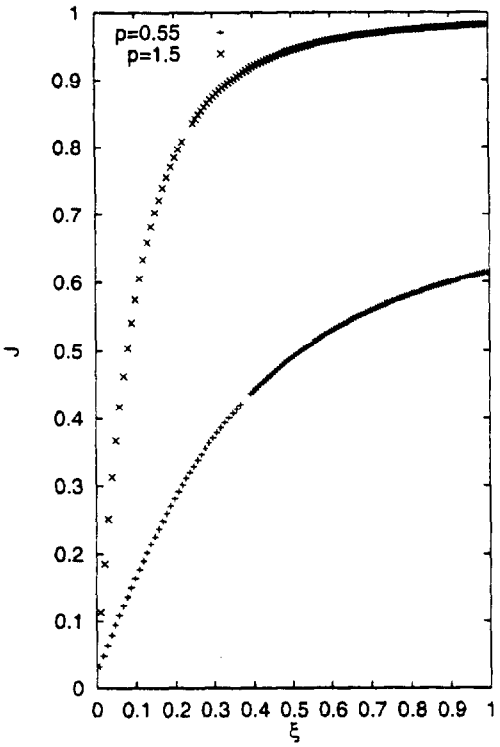

Fig. 4 The ion current

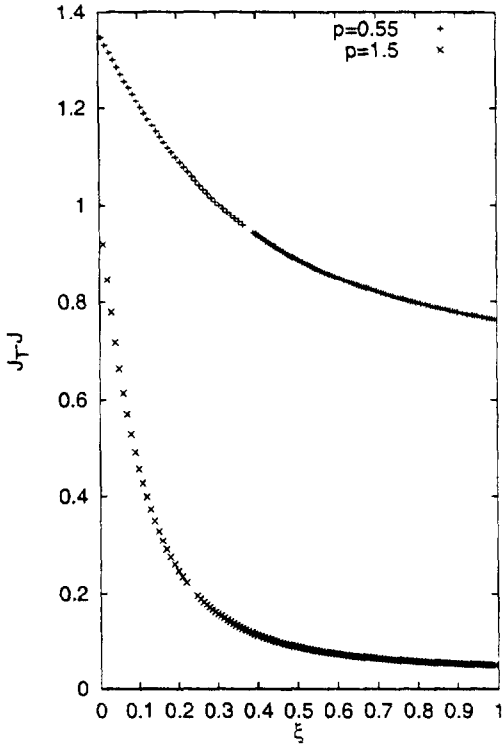

Fig. 6 The electron current

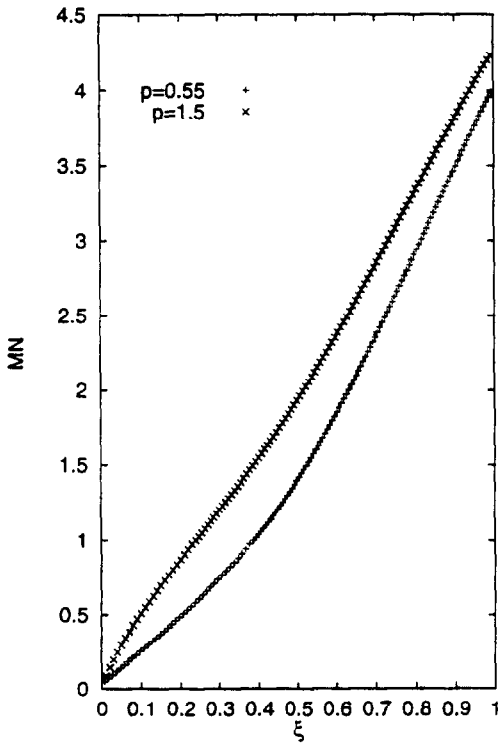

Fig. 5 The Mach number

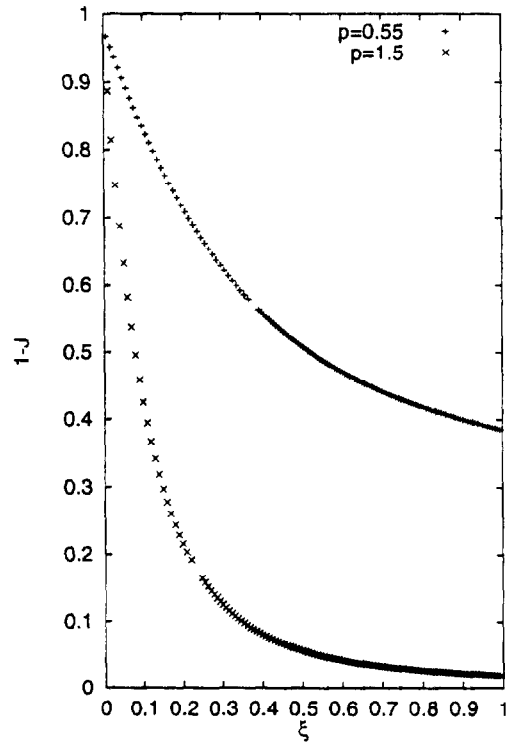

Fig. 7 The neutral density

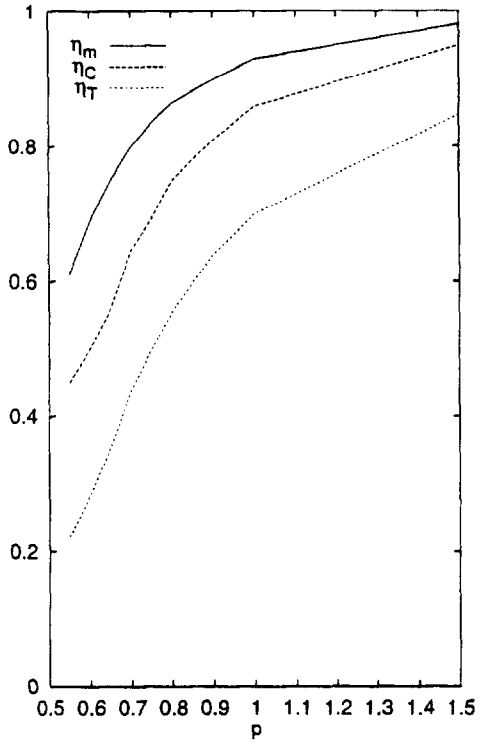

Fig. 8 Efficiencies as a function of p

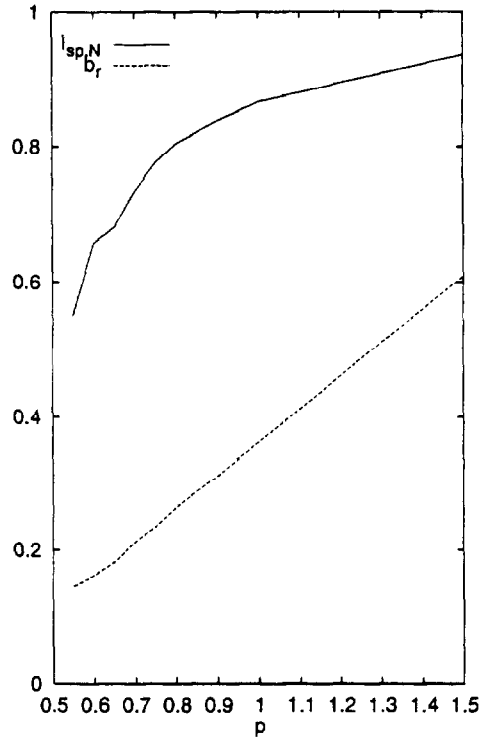

Fig. 9 The normalized specific impulse and magnetic field as a function of p

Note that the plasma density is peaked near the anode. This seems to be in disagreement with the measured density that peaks away from the anode. However, this difference might be traced to the assumption of a uniform electron temperature. Figure 5 shows the Mach number (MN) distribution. where $MN \equiv (J/N)/(2t)^{1/2}$. Figure 6 shows the electron current for the two cases; this current is much smaller when p is larger.

Figure 7 shows the profile of the neutral density. The neutral density falls as a function of the distance from the anode much faster for p larger. Figure 8 shows η_m, η_C, and η_T as a function of p. As shown in Fig. 9 μ_0 is varied simultaneously with the variation of p. Also shown in Fig. 9 is the normalized specific impulse $I_{sp,n}$ as a function of p.

V. Comparison with experimental results

We compare the theoretical calculations to the experimental parameter study performed at Soreq NRC.[10] The magnetic field profile in the experiment is similar to that shown in Fig. 1, which was used in the calculations. The Soreq experiment employed an applied voltage of 250 Volts, thruster cross section of 22 cm^2 and length of 20 mm, and a magnetic field of a characteristic intensity of 150G. The gas is Xenon and the mass flow rate was varied. To be sure, to compare the calculation presented in the previous section with experimental results, we need to know the experimental values of the parameter p and the function μ. While the geometrical dimensions A and L, the applied voltage ϕ_A, the ion and the electron mass, the mass flow rate and the gas velocity v_a are known, β is not known, mostly because the electron temperature is not known. We assume the following dependence of β on $\dot{m}$, a dependence that phenomenologically fits best to the experiment:

$$\beta = \frac{1.8 \cdot 10^{-7}}{1 + 2\dot{m}} , \qquad (10)$$

where $\dot{m}$ is expressed in mg/s and β is expressed in cm^3/s. This decrease of the ionization with an increase of $\dot{m}$ reflects a decrease in the electron temperature with the increase of the mass flow rate. The form (10) corresponds to electron temperature of about 15 eV for $\dot{m} = 0.85$ mg/s.

To proceed, we first compare the theoretically calculated η_m, η_c and η_T with the measured quantities. We then compare the theoretically calculated specific impulse, using Eq. (7f), with the experimentally measured specific impulse for these parameters.[13,17] The comparisons are shown in Figs. 10 and 11.

In Fig. 12 the experimental[17] and theoretical magnetic fields are compared. The experimental values shown are $I^{-1/2}$, where I is the current in Amperes flowing in the coils of the magnetic circuit.[17] The theoretical values are found by scaling the values of $\mu_0^{-1/2}$ until the theoretical and experimental values coincide for $\dot{m} \approx 1.4$ mg/s.

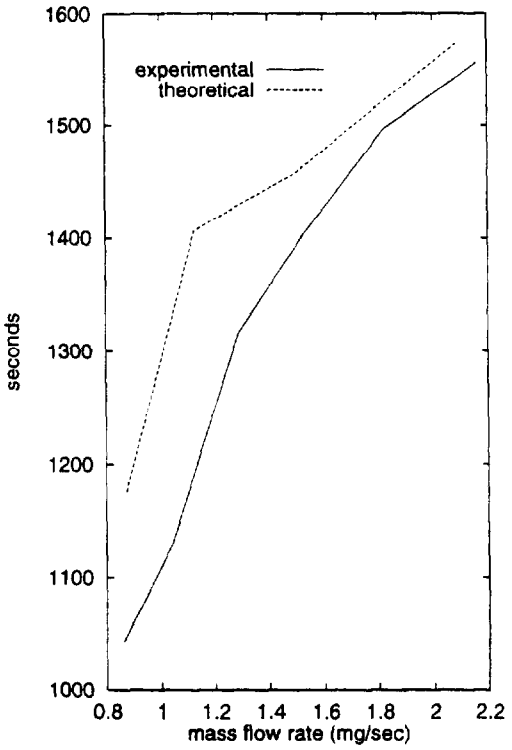

Fig. 11 Theoretical and experimental specific impulses

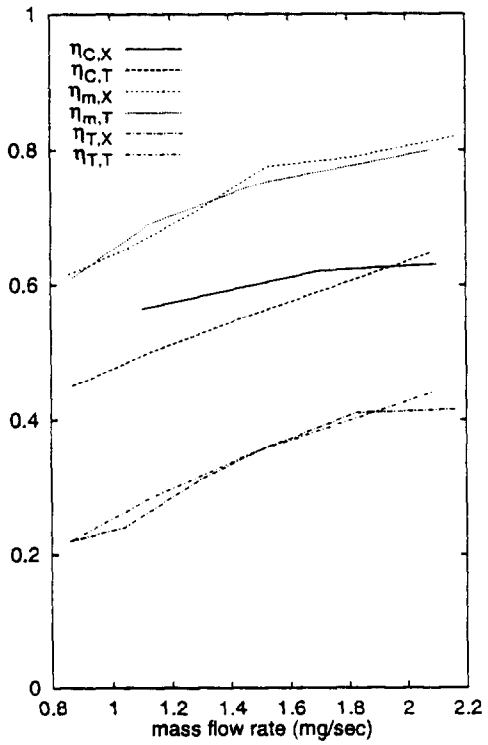

Fig. 10 Theoretical and experimental efficiencies

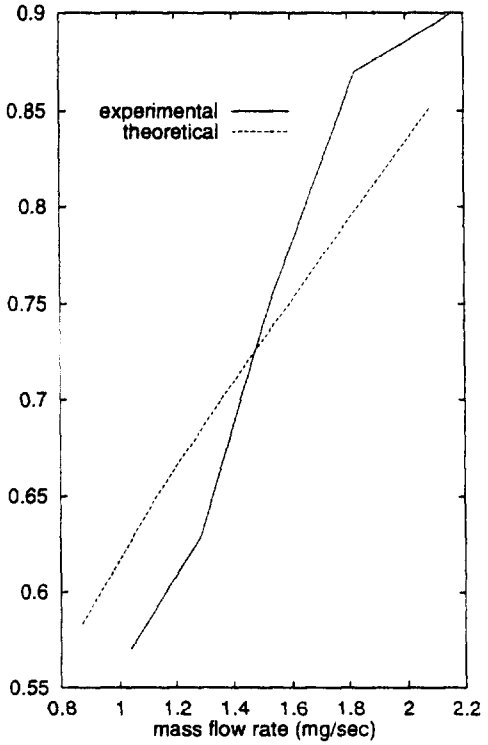

Fig. 12 Theoretical and experimental magnetic fields

VI. Summary

We have presented here a 1D steady–state model of a Hall thruster. We noted that the equations are singular at the sonic transition, and found regular solutions. The calculation agrees with experiment. The existence and uniqueness of the solutions will be examined in a subsequent study, where certain assumptions can be relaxed, including the cold fluid description of the ions, the uniform electron temperature, and the neglect of wall losses.

Acknowledgements

The research of A. F. and of N. J. F. has been partially supported by AFOSR.

References

1. Robert G. Jahn, "Physics of Electric Propulsion" (McGraw-Hill, New York, 1968), Chap. 8.
2. A. I. Morozov, Yu. V. Esipchuk, G. N. Ticinin, A. V. Trofinov, Yu. A. Sharov, and G. Ya. Shahepkin, "Plasma acceleration with closed electron drift and extended acceleration zone", Sov. Phys. Tech. Phys. **17**, 38 (1972).
3. A. I. Bugrova, A. I. Morozov, and V. K. Kharchevnikov,"Experimental investigation of near wall conductivity", Sov. J. Plasma Phys. **16**, 849 (1990).
4. K. Komurasaki, M. Hirakawa, and Y. Arakawa, "Plasma acceleration process in a Hall-current thruster", 22nd Int.EPC, Viareggio, Italy (1991), paper IEPC-91-078.
5. A. M. Bishaev, V. M. Gavryushin, A. I. Burgova, V. Kim, and V. K. Kharchvnikov, "The experimental investigations of physical processes and characteristics of stationary plasma thrusters with closed drift of electrons", 1st Russian-German EPC, Giessen, Germany, 1992. RGC-EP 92-06.
6. C. A. Lentz and M. Martinez-Sanchez, "Transient one dimensional numerical simulation of Hall Thrusters", AIAA paper 93-2491, Monterey, CA (1993).
7. E. Y. Choueiri, "Characterization of oscillations in closed drift thrusters", AIAA paper 94-3013. Indianapolis, IN (1994).
8. J. M. Fife and M. Martinez-Sanchez, "Two dimensional modeling of Hall thrusters". 3rd Russian-German EPC(page H44), Stuttgart, Germany, July 1994.
9. A. I. Morozov and V. V. Savelyev,"Numerical simulation of plasma flow in SPT". 24th Int. EPC, Moscow, Russia, 1995. IEPC-95-161.
10. J. Ashkenazy, Y. Raitses, and G. Appelbaum. "Investigations of a laboratory model Hall thruster", In 31^{st} JPC, San Diego, CA, USA. 1995. AIAA-95-2673.
11. D. H. Manzella, "Simplified numerical description of SPT operation", 24th Int. EPC, Moscow. Russia, 1995. IEPC-95-34.
12. M. Hirakawa and Y. Arakawa, "Numerical simulation of plasma particle behavior in a Hall thruster", In 32^{nd} JPC, Lake Buena Vista. FL. USA, 1996. AIAA-96-3195.
13. Y. Raitses, J. Ashkenazy, and M. Guelman. "Propellant utilization in Hall thrusters", In 32^{nd} JPC, Lake Buena Vista, FL, USA, 1996. AIAA-96-3193.
14. K. Komurasaki, K. Mikami, and D. Kusamoto. "Channel length and thruster performance of Hall thrusters", In 32^{nd} JPC, Lake Buena Vista. FL, USA, 1996. AIAA-96-3194.
15. V. Khayms and M. Martinez-Sanchez,"Design of a miniturized Hall thruster for microsatellites", In $32^{n}d$ JPC, Lake Buena Vista, FL. USA, 1996. AIAA-96-3291.
16. D. Oh and D. Hastings, "Experimental verification of a PIC-DSMC model for Hall thruster plumes", In 32^{nd} JPC, Lake Buena Vista, FL. USA, 1996. AIAA-96-3196.
17. Y. Raitses, Ph.D. thesis, 1997.